T1-Based Synthetic Magnetic Resonance Contrasts Improve Multiple Sclerosis and Focal Epilepsy Imaging at 7 T

Aurélien Massire, PhD,*† Charlotte Seiler, MD,*† Thomas Troalen, PhD,‡ Olivier M. Girard, PhD,*† Pierre Lehmann, MD, PhD,*†§ Gilles Brun, MD,*†§ Axel Bartoli, MD,*† Bertrand Audoin, MD, PhD,*†‖ Fabrice Bartolomei, MD, PhD,¶ Jean Pelletier, MD, PhD,*†‖ Virginie Callot, PhD,*† Tobias Kober, PhD,#**†† Jean-Philippe Ranjeva, PhD,*† and Maxime Guye, MD, PhD*†

***Aix-Marseille Univ, CNRS, CRMBM, Marseille, France; †APHM, Hôpital de la Timone, CEMEREM, Marseille, France; ‡Siemens Healthcare SAS, Saint-Denis, France; §Pôle d'Imagerie, Service de Neuroradiologie, ‖Pôle de Neurosciences Cliniques, Service de Neurologie, and ¶Pôle de Neurosciences Cliniques, Service de Neurophysiologie, APHM, Hôpital de la Timone, Marseille, France; #Advanced Clinical Imaging Technology, Siemens Healthcare AG, Lausanne, Switzerland; **Department of Radiology, Lausanne University Hospital and University of Lausanne, Lausanne, Switzerland; and ††Signal Processing Laboratory (LTS 5), École Polytechnique Fédérale de Lausanne (EPFL), Lausanne, Switzerland.**
Aurélien Massire and Charlotte Seiler contributed equally to this work.

Objectives: Ultra-high field magnetic resonance imaging (MRI) (≥7 T) is a unique opportunity to improve the clinical diagnosis of brain pathologies, such as multiple sclerosis or focal epilepsy. However, several shortcomings of 7 T MRI, such as radiofrequency field inhomogeneities, could degrade image quality and hinder radiological interpretation. To address these challenges, an original synthetic MRImethod based on T1 mapping achievedwith themagnetization-prepared 2 rapid acquisition gradient echo (MP2RAGE) sequencewas developed. The radiological quality of on-demand T1-based contrasts generated by this technique was evaluated in multiple sclerosis and focal epilepsy imaging at 7 T.

Materials and Methods: This retrospective study was carried out from October 2017 to September 2019 and included 21 patients with different phenotypes of multiple sclerosis and 35 patients with focal epilepsy who underwent MRI brain examinations using a whole-body investigative 7 T magnetic resonance system. The quality of 2 proposed synthetic contrast images were assessed and compared with conventional images acquired at 7 Tusing the MP2RAGE sequence by 4 radiologists, evaluating 3 qualitative criteria: signal homogeneity, contrast intensity, and lesion visualization. Statistical analyses were performed on reported quality scores using Wilcoxon rank tests and further multiple comparisons tests. Intraobserver and interobserver reliabilities were calculated as well.

Results: Radiological quality scores were reported higher for synthetic images when compared with original images, regardless of contrast, pathologies, or raters considered, with significant differences found for all 3 criteria ($P < 0.0001$, Wilcoxon rank test). None of the 4 radiologists ever rated a synthetic image **"**markedly worse**"** than an original image. Synthetic images were rated slightly less satisfying for only 3 epileptic patients, without precluding lesion identification.

Conclusion: T1-based synthetic MRI with the MP2RAGE sequence provided on-demand contrasts and high-quality images to the radiologist, facilitating lesion visualization in multiple sclerosis and focal epilepsy, while reducing themagnetic resonance examination total duration by removing an additional sequence.

Key Words: ultra-high field MRI, synthetic MRI, neuroradiology, epilepsy, multiple sclerosis, MP2RAGE, 7 T

Introduction

A core promise of ultra-high field (UHF) magnetic resonance imaging (MRI) (≥7 T) is to provide high-resolution images of normal and pathological anatomy of the human brain, thanks to higher intrinsic signal-to-noise ratio. Recent studies confirmed the clinical benefits of 7 T MRI1–5 and the added value of UHF in neurological diseases by comparing images obtained at 1.5 T, 3 T, and 7 T.6–8 As UHF MRI is hampered by radiofrequency field inhomogeneities and specific absorption rate increase, gradient echo (GRE) sequences quickly became the workhorse of UHF structural imaging.

The magnetization-prepared 2 rapid acquisition GREs (MP2RAGE9) was designed to provide field bias–free T1-weighted imaging at UHF10 and jointly achieve reliable T1 mapping. It has been consequently shown that MP2RAGE is superior to MPRAGE, providing better automated segmentation in normal brain.9,11,12 When used for multiple sclerosis (MS) imaging at 3 T13 and 7 T,14,15 MP2RAGE images showed higher sensitivity to MS lesion count (especially in the cortex) when compared with reference magnetic resonance (MR) sequences, while also enabling automated lesion detection and segmentation.16 Separately, MP2RAGE has also been identified as a key technique for UHF exploration of patients presenting focal epilepsy,17–19 notably by providing a clinically relevant "tissue border enhancement" contrast, useful for gray matter (GM)/white matter (WM) interface delineation and identification of cortical malformations.20

In addition, MP2RAGE parametrization could be changed to improve the visualization of cortical layers and deep structures.21,22 Fluid and white matter suppression (FLAWS23), an MP2RAGE sequence with specifically chosen inversion times, was thus introduced to provide a contrast with improved cortex and deep GM structure visualization, by taking the minimum intensity pixel (mIP) of the 2 inversion images to suppress bothWMand cerebrospinal fluid (CSF) signals. As a result, 7 T FLAWS imaging was considered superior, or at least complementary, to conventional T2-weighted 3-dimensional (3D) imaging for improved conspicuity of MS lesions24 and structural changes compatible with epileptogenic lesions,25 particularly, but not exclusively, in cases of normal appearing conventional MR at lower fields.17

However, a FLAWSparametrization loses MP2RAGE key properties, that is, reliable T1 mapping and immunity to field bias. More generally, obtaining optimal GM/WM visualization, additional clinically relevant contrast(s) such as GM/WM interface nulling or mIP FLAWS, and accurate T1 mapping only by running a single MP2RAGE acquisition with the aforementioned parametrizations9,21,23 is practically not feasible. Moreover, adding a FLAWS acquisition extends examination time. Therefore, we propose in this work to build multiple synthetic uniform MP2RAGE images with clinically relevant contrasts on-demand. To do so, MP2RAGE signal equations were reintegrated based on a single reliableMP2RAGE T1 map acquisition. Synthetic images were compared with conventional MP2RAGE/FLAWSimages acquired at 7 T by 4 radiologists on patients with MS and epilepsy, 2 key brain pathologies where 7 T MP2RAGE and FLAWS clinical benefits were already established.

MATERIALS AND METHODS

Population and MR Imaging

Twenty-one patients (18 women; age, 32 ± 7 [20–47] years; disease duration, 3 ± 1 [1–7] years; mean ± SD [range]) with different phenotypes of MS (according to the 2010 McDonald revised criteria) and 35 patients (20 women; age, 36 ± 10 [21–57] years; disease duration, 24 ± 12 [3–42] years; mean ± SD [range]) with drug-resistant focal epilepsy were recruited in this retrospective study. Both patient populations were recruited, between October 2017 and September 2019, froman ongoing distinct prospective study aiming to evaluate the added value of 7 Tover 3 Texplorations to characterizeMS and epileptogenic lesions. The exclusion criteria for both populations for the prospective study were alcohol or other drug abuse, history of psychiatric diseases, or any other neurologic diseases. No additional patients were excluded for this retrospective analysis. All MS patients (19 relapsing-remitting, 1 secondary progressive, and 1 primary progressive; see Supplementary Material Table A, http://links.lww.com/RLI/A562) underwent a standard neurologic examination by certified neurologists, and disability was assessed by the Expanded Disability Status Scale. All epilepsy patients were included in noninvasive presurgical evaluation and underwent interictal and ictal video-electroencephalogram recording. The protocol was approved by the local ethics committee and written consent was obtained from all subjects before the MR examinations. AllMS patients had 7 T MR-visible brain lesions. Twenty-one epilepsy patients had 7 T MRI abnormalities consistent with epileptogenic lesions (with diverse locations and lesion types, diagnosed on histological data in operated patients and on MRI criteria in nonoperated patients, see Supplementary Material Table B, http://links.lww.com/RLI/A562), whereas 14 epilepsy patients presented normal-appearing 7 T MRI. Experiments were performed using a whole-body investigative 7 T MR system (Magnetom 7 T, Siemens Healthcare, Erlangen, Germany), equipped with a 1Tx/32Rx head coil (Nova Medical, Wilmington, MA). A prototype MR sequence with 2 refocusing pulses generating a spin-echo and a stimulated echo was used to acquire low-resolution B1
+ maps. Two whole-brain 3D sagittal MP2RAGE acquisitions (T1 mapping and FLAWS, sequence parameters described in Table 1)were performed with a (0.6mm)3 isotropic resolution, a field of view of 240 mm (matrix size: 402 _ 402), 256 partitions, a parallel imaging acceleration factor of 3 (2D GRAPPA), and Partial Fourier factors of 6/8 in both phase- and partition-encoding directions. The first inversion image of the T1 mapping acquisition (henceforth called **“**EDGE**”** in this study) exhibited a clinically relevant **“**tissue border enhancement**”** at the GM/WM interface. The 2 inversion images of the FLAWS acquisition were merged with a mIP to obtain a clinically relevant GM hypersignal image (henceforth called **“**mIP FLAWS**”** in this study).

Synthetic MP2RAGE Theory

MP2RAGE is an inversion recovery-based 3D sequence where 2 GRE volumes are acquired at 2 different inversion times (TI1 and TI2) with 2 different flip angles (**α**1 and **α**2). By combining these 2 GRE volumes, a composite uniform T1-weighted image (UNI) can be generated:

$$\mathrm{UNI} = \frac{\mathrm{real}\left(\mathrm{GRE}^{*}_{\mathrm{TI1}}\mathrm{GRE}_{\mathrm{TI2}}\right)}{|\mathrm{GRE}_{\mathrm{TI1}}|^2+|\mathrm{GRE}_{\mathrm{TI2}}|^2},$$

where GRETI1 and GRETI2 are the complex signal intensities of the GRE volumes acquired at TI1 and TI2 and * is the complex conjugate operator. AUNI signal is always bound within the [−0.5; +0.5] range and ismainly T1-weighted, that is, with almost no

proton density, T2* and B1
− dependencies, which are canceled out.9
When resolving this equation, a direct relationship between UNI signal intensity and T1 values is found for any given voxel, hence providing T1 mapping capabilities to the sequence (see Appendix 1 in Marques et al9). Furthermore, assuming a perfect magnetization inversion, it could be highlighted that UNI signal is only a function of T1 and of 7 parameters: TI1, TI2, **α**1, **α**2, n, TR, and TRMP2R (with TRMP2R the sequence repetition time, n the number of partition-encoding steps, and TR the repetition time of GRE readout modules). By modifying these parameters and reinjecting actual T1 values into the UNI signal equation, the dynamic of UNI signal intensities with respect to T1 values can be fully controlled to change the contrast and retrospectively generate synthetic uniform images.

Synthetic MP2RAGE Processing

The MP2RAGE synthetic image processing first requires robust T1 mapping, achieved using an adapted MP2RAGE parametrization to sample the whole physiological T1 range. In addition, inaccurate T1 estimation caused by flip angle variations through the imaged volume at UHF could retrospectively be corrected by acquiring B1
+ maps and
reinjecting measured flip angles values in signal equation for each voxel.21,26,27 To do so, B1
+ maps were interpolated to MP2RAGE volumes resolution using the c3D reslice-identity function (ITK-SNAP, UPENN, Philadelphia, PA), and B1
+-inhomogeneity correction was performed in MATLAB (The Mathworks, Natick, MA). T1 maps were denoised using a block-matching and filtering algorithm28 to reduce noise propagation to synthetic UNI images.9 The MP2RAGE synthetic parameters were chosen empirically (see Table 2 and Fig. 1) to generate 2 synthetic images with both clinically relevant contrast and uniform property:
-**“**sEDGE**”** stands for **“**synthetic EDGE**”** and consists in nulling the signal of voxels which contain about 50/50% of GM/WM, that is, with a T1 value of about 1600 milliseconds at 7 T.29 Synthetic EDGE images therefore exhibit a dark GM/WM border and will be compared with conventional EDGE images.
-**“**sFLAWS**”** stands for **“**synthetic FLAWS**”** and consists in nulling the signal of voxelswhich mainly contain eitherWM(T1 ~1200milliseconds) or CSF (T1 >3000 milliseconds). To do so, 2 synthetic uniformimageswere generated: sFLAWS1 (WMnulling) and sFLAWS2 (CSF nulling). Both images were merged to obtain a mIP image (sFLAWS) using MATLAB (for each voxel, sFLAWS value corresponds to the smallest value between sFLAWS1 and sFLAWS2). Synthetic FLAWS images therefore exhibit GM hypersignal and will be compared with conventional mIP FLAWS images.
The MATLAB code for calculating sEDGE and sFLAWS images is available for download on request to the corresponding author.

Radiological Assessment and Clinical Data Analyses

All images were skull-stripped using BET (FSL v4.1.3; FMRIB, Oxford, UK). Acquired and synthetic images were interpreted by 4 radiologists who had access to patient clinical data: 2 senior neuroradiologists

(G.B. and P.L., with 5 and 20 years of experience as registered neuroradiologists, respectively) and 2 residents (C.S. and A.B., fifth year of radiological residency). EDGE images were compared to sEDGE images, whereas mIP FLAWS images were compared to sFLAWS images. For each patient, original and synthetic series of imageswere randomly renamed to avoid evaluation bias (**"**techniqueA**"** or **"**technique B**"** for EDGE/sEDGE; **"**technique C**"** or **"**technique D**"** for mIP FLAWS/sFLAWS). Images were rated by evaluating 3 qualitative criteria: signal homogeneity (through the whole brain), apparent contrast (between GM/WM/CSF, and their interfaces), and proper visualization of pathological lesions/features. In epileptic patients without visible lesions on any images, the last criterion was not rated. For each criterion, techniqueA/C qualitywas always rated relatively to technique B/D, using a 5-point relative scale ranging from−2 to +2, with −2,markkedly worse; −1, slightly worse; 0, equivalent; +1, slightly better; +2, markedly better. Grades were retrospectively sorted to rate synthetic images performances according to original images.

Statistical analyses were performed using JMP9 (SAS institute, Cary, NC). Quality scores comparisons were performed using Wilcoxon rank tests (P values <0.05were considered as statistically significant). Multiple comparisons were carried out using a paired analysis of variance followed by post hoc Steel-Dwass nonparametric tests (Bonferroni corrected for multiple comparisons). To evaluate interobserver reliability, Fleiss κ coefficient was calculated merging the 5-point scale into 2 groups: superior or equal (+2/+1/0) and inferior (−1/−2). Intraobserver reproducibility was assessed using Cohen κ coefficient, with rater 1 (C.S.) interpreting all images a second time, with a period of 5 days between analyses.

RESULTS

Figure 1a shows the relationships between T1 values and UNI signal intensities for T1 mapping (black) and FLAWS (blue) MP2RAGE protocols. The decrease of the black curve is monotonous for the physiological T1 range, granting reliable T1 mapping. However, the blue curve goes markedly upward before bending around the T1 ~2000 millisecond range. Consequently, it provides ambiguous T1 mapping for GM voxels, illustrating the fact that the UNI image generated by the FLAWS protocol is not usable in practice for T1 mapping.

Figure 1b shows synthetic UNI signal dynamics versus T1 values for synthetic MP2RAGE protocols: sEDGE (green) and sFLAWS (red; the mIP between sFLAWS1 and sFLAWS2 is illustrated with dashed lines). The parameter choice for MP2RAGE resulted in WM and CSF voxels exhibiting the lowest (ie, nulled) signal in sFLAWS images and voxels in the range of 1500 to 1700 milliseconds exhibiting the lowest (ie, nulled) signal in sEDGE images, respectively.

When pooling rates from all raters and patients, the quality scores of the sEDGE images were significantly higher than those of the original EDGE images ($P < 0.0001$, Wilcoxon rank test) for the 3 qualitative criteria, namely, signal homogeneity (median, 1; range, −1 to 2), apparent contrast (median, 2; range, −1 to 2), and lesion visualization (median, 1; range, −1 to 2). Significantly higher quality ratings ($P < 0.0001$, Wilcoxon rank test) were also obtained for sFLAWS images compared with acquired mIP FLAWS images with median signal homogeneity scores of 2 (range, 0 to 2), median apparent contrast scores of 2 (range, 0 to 2), and median lesion visualization scores of 1

(range, −1 to 2). Relative grades distributions for each pathology and contrast are displayed in Figure 2.

One paired analysis of variance conducted on all relative scores showed a significant effect of rating scores among criteria ($F = 64.77$, $P < 0.0001$), a significant (scores _ pathology) interaction ($F = 8.52$, $P < 0.0001$), and a significant (scores _ raters) interaction ($F = 3.85$, $P < 0.0001$). Post hoc testing showed significantly higher scores for MS relative to epilepsy when considering lesion visualization on sFLAWS (mean ± SD: MS, 1.31 ± 0.66; epilepsy, 0.61 ± 0.91; $P = 0.0006$) and on sEDGE (mean ± SD: MS, 1.02 ± 0.58; epilepsy, 0.67 ± 0.78; $P = 0.0066$).

Concerning the rater effect, calculated intraobserver and interobserver agreements were as follows: Kintra = 0.81 and Kinter = 0.70, respectively. In addition, post hoc testing showed significantly lower contrast quality scores given by 1 rater compared with 2 others for sFLAWS (1.39 ± 0.71 vs 1.75 ± 0.48 [$P = 0.0182$] and 1.82 ± 0.43 [$P = 0.0012$], Steel-Dwass test) and for sEDGE (1.23 ± 0.74 vs 1.55 ± 0.74 [$P = 0.0198$] and 1.55 ± 0.74 [$P = 0.0198$] Steel-Dwass test). The rater with lowest scoring was not the same for the 2 different contrasts (1 junior for sFLAWS, 1 senior for sEDGE; see Supplementary Material Table C, http://links.lww.com/RLI/A562

None of the 4 radiologists ever rated a synthetic image **“**markedly worse**”** (−2) than an original image. However, 1 patient's sEDGE image and 2 patients' sFLAWS images were unanimously rated **“**slightly worse**”** for epileptic lesion visualization (for all cases, lesions could still be depicted in synthetic images, see for details).

Figure 3 illustrates representative cases where synthetic image contrast intensity and signal homogeneity were considered significantly improved when compared with originally acquired images. Because synthetic images are uniform images computed from T1 maps, signal is maintained in temporal lobes (Fig. 3a), enabling improved visualization of pathological features in these regions. Uniform images are also field bias-free, which is clearly visible in the occipital region in Figure 3b. As for image contrast, sEDGE exhibits brighter WM signal and sharper GM/WM signal nulling than EDGE. The GM/WM contrast in sFLAWS is increased compared with conventional FLAWS, with more efficient WM signal nulling.

Representative images obtained on MS patients are shown in Figure 4. Visualization of cortical, subcortical, and WM MS lesions was improved using synthetic contrasts, when comparedwith their originally acquired counterparts. Visualization of MS lesion was enhanced on synthetic images because of improved tissue contrast and signal homogeneity, especially at cortical and subcortical locations (Fig. 4a and b). The signal gain on synthetic images in the posterior fossa allowed for an improved visualization of the MSlesion located on the brainstem, poorly seen on conventional images (Fig. 4c).

Resulting images for 2 representative epilepsy patients are shown in Figure 5. In epilepsy, focal cortical dysplasia (FCD), associated to abnormal T1 value range, exhibited blurred WM/GM junction, cortical thickness alterations, and gyration anomalies. Focal cortical dysplasia could be easily visualized on synthetic images (yellow arrows), which were considered superior (Fig. 5a) or equivalent (Fig. 5b) to conventional images. The **“**transmantle sign,**”** typical of FCD type IIb, is visible on these images (blue arrows).

Figure 6 shows individual cases where synthetic images were considered slightly inferior than their original counterparts for lesion visualization. Figure 6a illustrates a case of a type IIb FCD with less obvious cortical thickening in an sFLAWS image. The diagnosis information is nonetheless maintained in sFLAWS, as the transmantle sign is visible on the sagittal view. Figure 6b illustrates another FCD IIb where an sEDGE image was rated slightly inferior for WM-lesion contrast. Again, the transmantle sign is still visible in sEDGE. Figure 6c shows a patientwith polymicrogyria, where the compacted aspect of the parenchyma in sFLAWS image was considered slightly less visually informative than in original mIP FLAWS image. Still, all radiologists confirmed that the polymicrogyria delineation was clinically acceptable in sFLAWS and that the diagnosis information was preserved.

DISCUSSION

The MP2RAGE sequence is well suited for UHF brain imaging, benefiting from intrinsic volume coregistration, relative immunity to inhomogeneous field bias, and low specific absorption rate.9,21 It also provides reliable T1 measurements as a surrogate in vivo biomarker of microstructural changes,30 but with a still limited added value for clinical assessment, as the information contained in T1 maps is not readily usable for radiologists yet. To still benefit from this valuable quantitative information and to correct all images for signal bias and imperfect contrast, a new technique called synthetic MP2RAGE was introduced and validated to generate images derived from unbiased T1 maps and which consequently exhibited uniform, mainly T1-based signal and contrast in the brain. Using the proposed synthetic framework, tissue contrast could be manipulated nonlinearly (ie, nulled, compressed, extended, or highlighted) according to many specific clinical needs. This technique only requires changing retrospectively MP2RAGE key parameters, such as inversion times or flip angles, and reintegrating sequence signal equations to generate a synthetic UNI image, to provide a 2-fold benefit. First, highly contrasted and uniform images are generated, with restored signal in temporal lobes, brainstem, and posterior fossa, presumably allowing the visualization of potential lesions that cannot be easily visible on conventionally acquired images. Second, this synthetic MP2RAGE framework allows shortening the MRI examination time by saving the 10-minute duration of a 600-μm isotropic resolution FLAWS acquisition (now superfluous), which is a significant asset to consider for UHF high-resolution examination design. In this study, MP2RAGE protocol parameters were empirically chosen to obtain synthetic images with a signal intensity profile with respect to T1 values aimed at improving the contrast between structures of interest while being comparable to a certain extent with 2 clinically relevant contrasts, based on current literature14–25 and the authors' own experience. In the future, profit functions31 could be used to optimize MP2RAGE parameters and further improve synthetic image contrast and diagnosis potential to address various clinical questions, such as WM T1 signal suppression in developing brain.

The results obtained in this study largely supported the radiological subjective preference of synthetic MP2RAGE images over conventionally acquired MP2RAGE images in terms of signal homogeneity and contrast intensity. Improvement in signal homogeneity and contrast within the infratentorial region, which is a frequent and typical location

of MS lesion included in the McDonald criteria, was demonstrated. In addition, 14 of 21 patients exhibited cortical MS lesions. As cortical involvement in MS is correlated with the progression of cognitive disorders and clinical deficits and related to irreversible clinical damage,[32,33] the increased spatial resolution of UHF synthetic MP2RAGE images is a major asset to characterize MS lesions.[14,34] On the other hand, malformations of cortical development identification and characterization is a major issue in drug-resistant focal epilepsy, as well as a central key to surgical success.[35] The epilepsy cohort examined in this work was representative of the usual distribution of malformations of cortical development, with a majority of FCD. The "blurredGM/WMjunction" (particularly visible on EDGE/sEDGE), which is a typical feature of FCD on MRI,[25] and the "transmantle sign" (particularly visible on mIP FLAWS/sFLAWS), which is (1) typical of FCD type IIb,[36] (2) may also be seen in other FCD subtypes, and (3) has better postoperative prognosis for seizure control,[37] were both clearly identified on synthetic MP2RAGE images. Thus, the proposed method could be used not only to shorten scanning time but also has the potential to improve radiological interpretation of 7 T images, both in MS and focal epilepsy.

Several limitations of this study should be acknowledged, as image quality radiological assessment is inherently subjective. Firstly, the goal of the presented radiological assessment was to preliminary evaluate a methodological innovation by determining if synthetic images could be easier to read by several raters with various experience levels. For the sake of simplicity and after a consensus, the radiologists decided to compare original and synthetic images using a simultaneous but blinded display of the 4 images with a random quadrant positioning, 3 qualitative criteria, and a 5-point relative rating scale, rather than performing 2 independent ratings.[38,39] Although already informative, such method design cannot readily be applied to evaluate lesion depiction (ie, detection/identification) and derive subsequent clinical added benefit. Indeed, as all 4 images were simultaneously shown to the rating radiologist, some lesions could have been implicitly identified via coregistration to the "best" image at hand. Second, an overall strong agreement was found between the radiologists, as well as a high intraobserver reproducibility. However, several significant differences in scoring between junior and senior raters were found especially for the sFLAWS technique, which likely indicates that each rater reacted differently to this contrast. A possible explanation would be the experience already acquired before this study by senior radiologists with regard to the interpretation of 7 T images, which definitely requires a period of learning and an adaptation of radiological practices. Nevertheless, this rating difference did not affect the interpretation. With regard to possible lesion identification and characterization missing using the synthetic MP2RAGE technique, only a handful of cases were judged slightly less visually satisfying than originally acquired images on the whole cohort. Although no perfect score was indeed reached, it should be noted that synthetic image clinical interpretation (ie, lesion identification and characterization) was always considered possible by the radiologists, accounting for the simultaneous display limitation stated above. Contrast ratio measurements between regions of interest would have been possible, likely showing synthetic contrasts superiority as these imageswere generated with the aimto maximize thismetric. However, the authors felt that the qualitative nature of the radiologist

evaluation was eventually the most relevant criterion.
In conclusion, this study provides new evidences onMP2RAGE sequence usefulness in neuroradiology, when studying MS and focal epilepsy at UHF. As UHF 3D acquisitions with high isotropic spatial resolution are usually very long, new methods such as the herein presented synthetic MP2RAGE technique and subsequent adaptation of radiological practices are both required to reduce total examination time, while trying to provide improved image quality. Independent, comprehensive, and quantitative assessments will be required in the future to demonstrate a direct clinical benefit of synthetic images. Still, with no extra acquisition time needed and fast image postprocessing (synthetic signal calculation takes only a few seconds on a standard computer, making online display at theMR system possible), synthetic MP2RAGE successfully provided clinically relevant T1-based contrasts to the radiologist for improved pathological brain visualization. Lastly, this technique is not specific to 7 T imaging and could be readily translated to clinical 3 T MP2RAGE imaging.

Conflicts of interest and sources of funding: This study was supported by the following funding sources: 7T-AMI ANR-11-EQPX-0001, A*MIDEX-EI-13-07-130115-08.38-7T-AMISTART, Fondation ARSEP (Fondation pour l'Aide à la recherche sur la Sclérose en Plaques), and CNRS (Centre National de la Recherche Scientifique). Dr Massire is an employee of Siemens Healthcare SAS since September 2019. Dr Troalen is currently an employee of Siemens Healthcare SAS. Dr Kober is a current employee and shareholder of Siemens Healthcare AG and holds patents filed by Siemens Healthcare. For the remaining authors, no relevant relationships are declared.

REFERENCES

1. Kraff O, Fischer A, Nagel AM, et al. MRI at 7 tesla and above: demonstrated and potential capabilities. J Magn Reson Imaging. 2015;41:13–33.
2. Trattnig S, BognerW, Gruber S, et al. Clinical applications at ultrahigh field (7 T): where does it make the difference? NMR Biomed. 2016;29:1316–1334.
3. van der Kolk AG, Hendrikse J, Zwanenburg JJM, et al. Clinical applications of 7T MRI in the brain. Eur J Radiol. 2013;82:708–718.
4. Trattnig S, Springer E, Bogner W, et al. Key clinical benefits of neuroimaging at 7T. Neuroimage. 2018;168:477–489.
5. Düzel E, Acosta-Cabronero J, Berron D, et al. European Ultrahigh-Field Imaging Network for Neurodegenerative Diseases (EUFIND). Alzheimers Dement (Amst). 2019;11:538–549.
6. Obusez EC, Lowe M, Oh S-H, et al. 7TMRof intracranial pathology: preliminary observations and comparisons to 3T and 1.5T. Neuroimage. 2018;168:459–476.
7. Springer E, Dymerska B, Cardoso PL, et al. Comparison of routine brain imaging at 3 T and 7 T. Invest Radiol. 2016;51:469–482.
8. Kollia K, Maderwald S, Putzki N, et al. First clinical study on ultra-high-field MR imaging in patients with multiple sclerosis: comparison of 1.5Tand 7T. AJNR Am J Neuroradiol. 2009;30:699–702.
9. Marques JP, Kober T, Krueger G, et al. MP2RAGE, a self bias–field corrected sequence for improved segmentation and T1-mapping at high field. Neuroimage. 2010;49:1271–1281.
10. Van de Moortele P-F, Auerbach EJ, Olman C, et al. T1 weighted brain images at 7 tesla unbiased for proton density, T2* contrast and RF coil receive B1 sensitivity with simultaneous vessel visualization. Neuroimage. 2009;46:432–446.
11. Choi U-S, Kawaguchi H, Matsuoka Y, et al. Brain tissue segmentation based on

MP2RAGE multi-contrast images in 7 T MRI. PLoS One. 2019;14:e0210803.
12. O'Brien KR, Kober T, Hagmann P, et al. Robust T1-weighted structural brain imaging and morphometry at 7T using MP2RAGE. PLoS One. 2014;9:e99676.
13. Kober T, Granziera C, Ribes D, et al. MP2RAGE multiple sclerosis magnetic resonance imaging at 3 T. Invest Radiol. 2012;47:346–352.
14. Beck ES, Sati P, Sethi V, et al. Improved visualization of cortical lesions in multiple sclerosis using 7T MP2RAGE. AJNR Am J Neuroradiol. 2018;39:459–466.
15. Kolber P, Droby A, Roebroeck A, et al. A **"**kissing lesion**"**: in-vivo 7T evidence of meningeal inflammation in earlymultiple sclerosis. Mult Scler. 2017;23:1167–1169.
16. Fartaria MJ, Sati P, Todea A, et al. Automated detection and segmentation of multiple sclerosis lesions using ultra-high-field MP2RAGE. Invest Radiol. 2019;54: 356–364.
17. Guye M, Bartolomei F, Ranjeva JP. Malformations of cortical development: the role of 7-tesla magnetic resonance imaging in diagnosis. Rev Neurol. 2019;175: 157–162.
18. Feldman RE, Delman BN, Pawha PS, et al. 7T MRI in epilepsy patients with previously normal clinicalMRI exams compared against healthy controls. PLoS One. 2019;14:e0213642.
19. Pittau F, BaudMO, Jorge J, et al. MP2RAGE and susceptibility-weighted imaging in lesional epilepsy at 7T. J Neuroimaging. 2018;28:365–369.
20. CostagliM, Kelley DAC, Symms MR, et al. Tissue border enhancement by inversion recovery MRI at 7.0 tesla. Neuroradiology. 2014;56:517–523.
21. Marques JP, Gruetter R. New developments and applications of the MP2RAGE sequence—focusing the contrast and high spatial resolution R1 mapping. PLoS One. 2013;8:e69294.
22. SudhyadhomA, Haq IU, FooteKD, et al. A high resolution and high contrastMRI for differentiation of subcortical structures for DBS targeting: the fast gray matter acquisition T1 inversion recovery (FGATIR). Neuroimage. 2009;47(suppl 2): T44–T52.
23. Tanner M, Gambarota G, Kober T, et al. Fluid and white matter suppression with the MP2RAGE sequence. J Magn Reson Imaging. 2012;35:1063–1070.
24. Urushibata Y, Kuribayashi H, Fujimoto K, et al. Advantages of fluid and white matter suppression (FLAWS) with MP2RAGE compared with double inversion recovery turbo spin echo (DIR-TSE) at 7T. Eur J Radiol. 2019;116:160–164.
25. Chen X, Qian T, Kober T, et al. Gray-matter-specific MR imaging improves the detection of epileptogenic zones in focal cortical dysplasia: a new sequence called fluid and white matter suppression (FLAWS). NeuroImage Clin. 2018;20: 388–397.
26. Haast RAM, Ivanov D, Uludağ K. The impact of B1+ correction on MP2RAGE cortical T 1 and apparent cortical thickness at 7T. Hum Brain Mapp. 2018;39: 2412–2425.
27. Massire A, Taso M, Besson P, et al. High-resolution multi-parametric quantitative magnetic resonance imaging of the human cervical spinal cord at 7T. Neuroimage. 2016;143:58–69.
28. Maggioni M, Katkovnik V, Egiazarian K, et al. Nonlocal transform-domain filter for volumetric data denoising and reconstruction. IEEE Trans Image Process. 2013;22:119–133.
29. Caan MWA, Bazin PL, Marques JP, et al. MP2RAGEME: T 1, T 2 *, and QSM mapping in one sequence at 7 tesla. Hum Brain Mapp. 2019;40:1786–1798.
30. Simioni S, Amarù F, Bonnier G, et al. MP2RAGE provides new clinically-compatible correlates of mild cognitive deficits in relapsing-remitting multiple sclerosis. J Neurol. 2014;261:1606–1613.
31. Beaumont J, Saint-Jalmes H, Acosta O, et al. Multi T1-weighted contrast MRI with fluid and white matter suppression at 1.5 T. Magn Reson Imaging. 2019; 63:217–225.

32. Louapre C, Bodini B, Lubetzki C, et al. Imaging markers of multiple sclerosis prognosis. Curr Opin Neurol. 2017;30:231–236.
33. Treaba CA, Granberg TE, Sormani MP, et al. Longitudinal characterization of cortical lesion development and evolution in multiple sclerosis with 7.0-T MRI. Radiology. 2019;291:740–749.
34. Heckova E, Strasser B, Hangel GJ, et al. 7 T magnetic resonance spectroscopic imaging in multiple sclerosis: how does spatial resolution affect the detectability of metabolic changes in brain lesions? Invest Radiol. 2018;54:247–254.
35. Oluigbo CO, Wang J, Whitehead MT, et al. The influence of lesion volume, perilesion resection volume, and completeness of resection on seizure outcome after resective epilepsy surgery for cortical dysplasia in children. J Neurosurg Pediatr. 2015;15:644–650.
36. Mellerio C, Labeyrie M-A, Chassoux F, et al. Optimizing MR imaging detection of type 2 focal cortical dysplasia: best criteria for clinical practice. AJNR Am J Neuroradiol. 2012;33:1932–1938.
37. Wang DD, Deans AE, Barkovich AJ, et al. Transmantle sign in focal cortical dysplasia: a unique radiological entity with excellent prognosis for seizure control. J Neurosurg. 2013;118:337–344.
38. Finck T, Li H, Grundl L, et al. Deep-learning generated synthetic double inversion recovery images improve multiple sclerosis lesion detection. Invest Radiol. 2020; 55:318–323.
39. Eichinger P, Hock A, Schön S, et al. Acceleration of double inversion recovery sequences in multiple sclerosis with compressed sensing. Invest Radiol. 2019;54: 319–324.

TABLES

MP2RAGE Acq.	TA, min s	TR_{MP2R}, s	α_1, °	α_2, °	TI_1, ms	TI_2, ms	TR, ms	TE, ms	BW, Hz/Px
T_1 mapping	10.12	5	6	5	900	2750	7.4	3.13	240
FLAWS	10.12	5	4	5	650	1700	5.1	2.2	430

Abbreviations: FLAWS, fluid and white matter suppression; MP2RAGE, magnetization-prepared 2 rapid acquisition gradient echo; TR, repetition time; TR_{MP2R}, sequence repetition time; TA, acquisition time; TE, echo time; BW, bandwidth per pixel.

TABLE 1. Sequence Parameters for MP2RAGE Acquisitions (T_1 Mapping and FLAWS) Used in This Study

MP2RAGE Synthetic Protocols	TR_{MP2R}, s	α_1, °	α_2, °	TI_1, ms	TI_2, ms	TR, ms
sEDGE	8	5	5	820	1320	2.5
$sFLAWS_1$	8.25	9	5	900	3700	7.5
$sFLAWS_2$	5	5	5	200	1200	3.1

Abbreviations: MP2RAGE, magnetization-prepared 2 rapid acquisition gradient echo; sEDGE, synthetic EDGE; sFLAWS, synthetic fluid and white matter suppression; TR, repetition time; TR_{MP2R}, sequence repetition time.

TABLE 2. MP2RAGE Sequence Parameters Used to Generate Synthetic Images (sEDGE, $sFLAWS_{1/2}$) Used in This Study

FIGURES

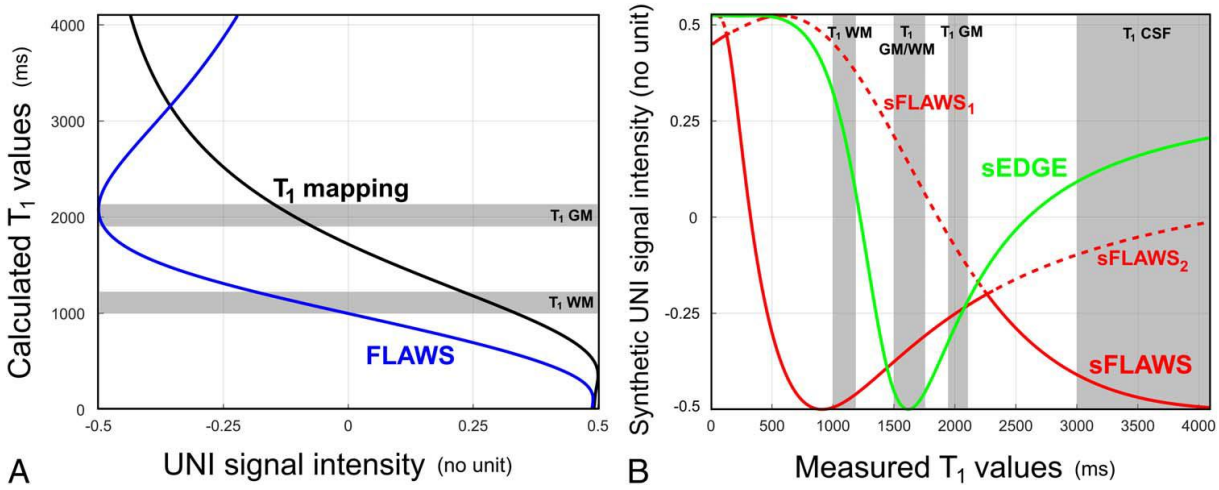

FIGURE 1. A, Evaluated T_1 values (output) versus UNI signal intensity dynamics (input) for "T_1 mapping" (black) and "FLAWS" (blue) MP2RAGE protocols, both originally acquired on patients. Only the black curve is relevant for T_1mapping, as itmonotonously samples the physiological T_1 range. B, Generated UNI signal intensities (output) versus input T_1 values for synthetic MP2RAGE protocols: sEDGE (green) and sFLAWS (red). Approximate T_1 ranges corresponding to brain GM and WM, as well as CSF, are also illustrated with gray areas. The lowest value of −0.5 corresponds to a dark (ie, nulled) signal intensity in the images.

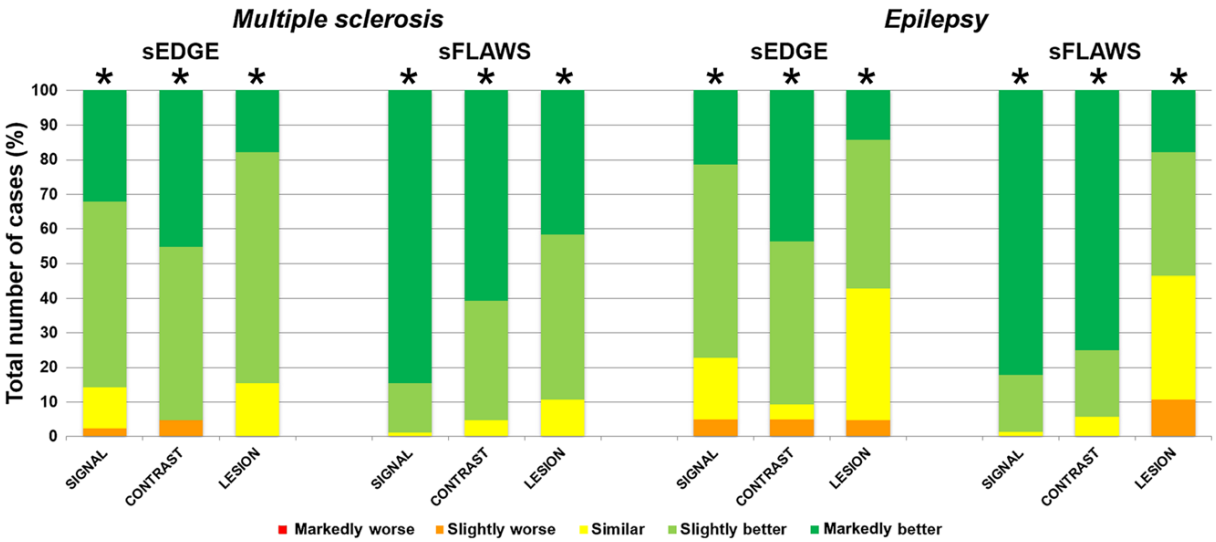

*FIGURE 2. Results of the radiological comparison between originally acquired and synthetic images. Radiologists' rates were combined into relative distributions (in percentage of total number of cases) for the 3 assessed criteria (signal homogeneity, contrast intensity, lesion visualization). For each pathology (multiple sclerosis and epilepsy): sEDGE rating versus EDGE (left); sFLAWS rating vs mIP FLAWS (right). Relative quality scores of synthetic images were significantly higher (marked with *) than original images (P < 0.0001, Wilcoxon rank test) for the 3 qualitative criteria.*

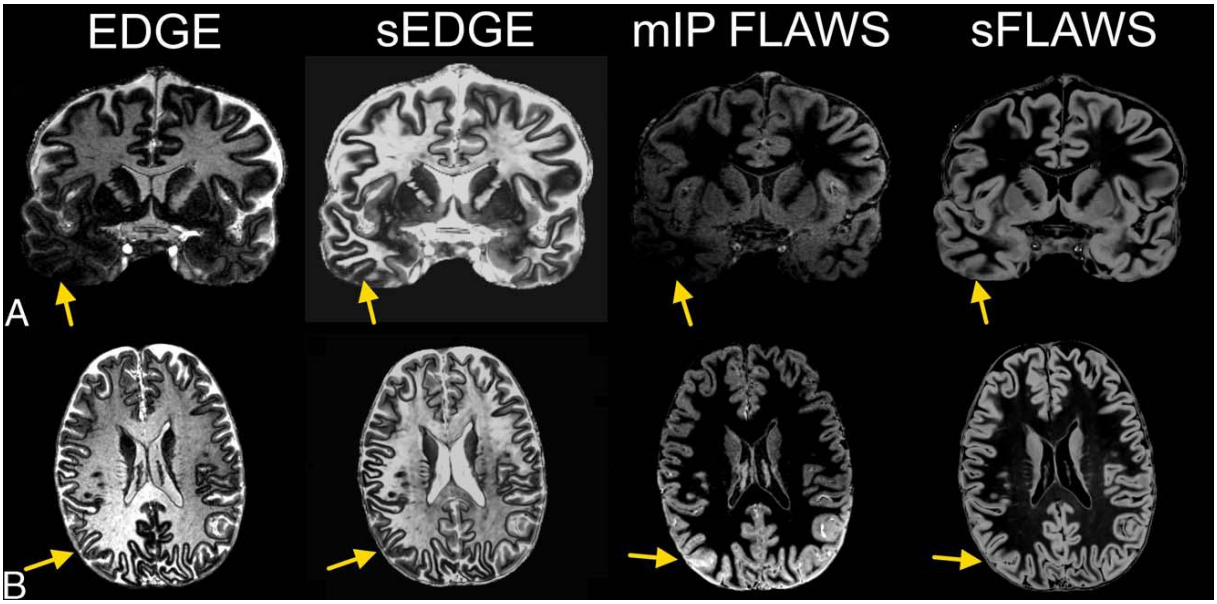

FIGURE 3. Signal homogeneity and contrast intensity improvements of synthetic images. A, Signal homogeneity improvements in temporal lobes (yellow arrows, coronal views). B, Field bias suppressions in synthetic images (yellow arrows, axial views). For each case, fromleft to right: EDGE, sEDGE, mIP FLAWS, and sFLAWS images.

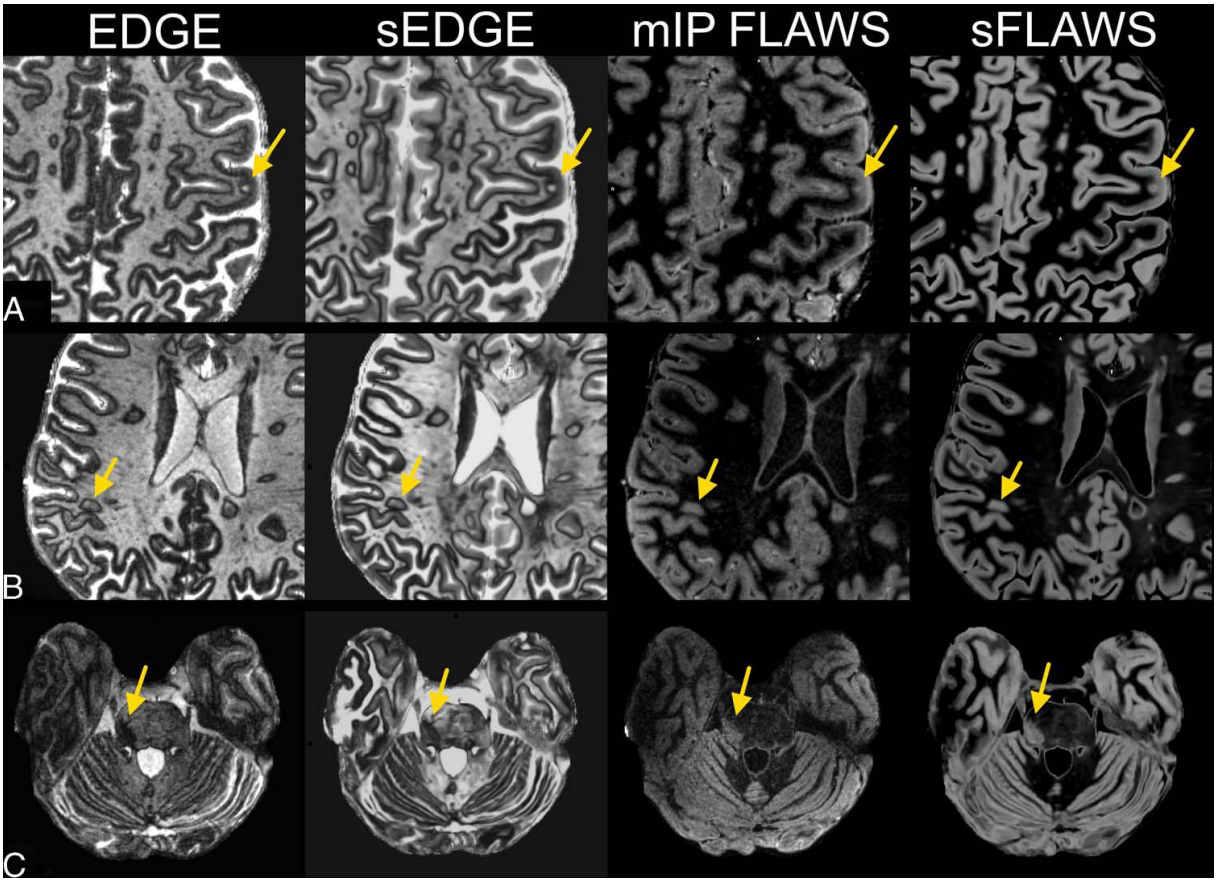

FIGURE 4. Multiple sclerosis 7 T imaging using MP2RAGE, with improved visualization of MS lesions on synthetic images, when compared to originally acquired images. Representative examples of (A) cortical, (B) mixed, and (C) infratentorial MS lesions (yellow arrows). For each case, from left to right: EDGE, sEDGE, mIP FLAWS, and sFLAWS images.

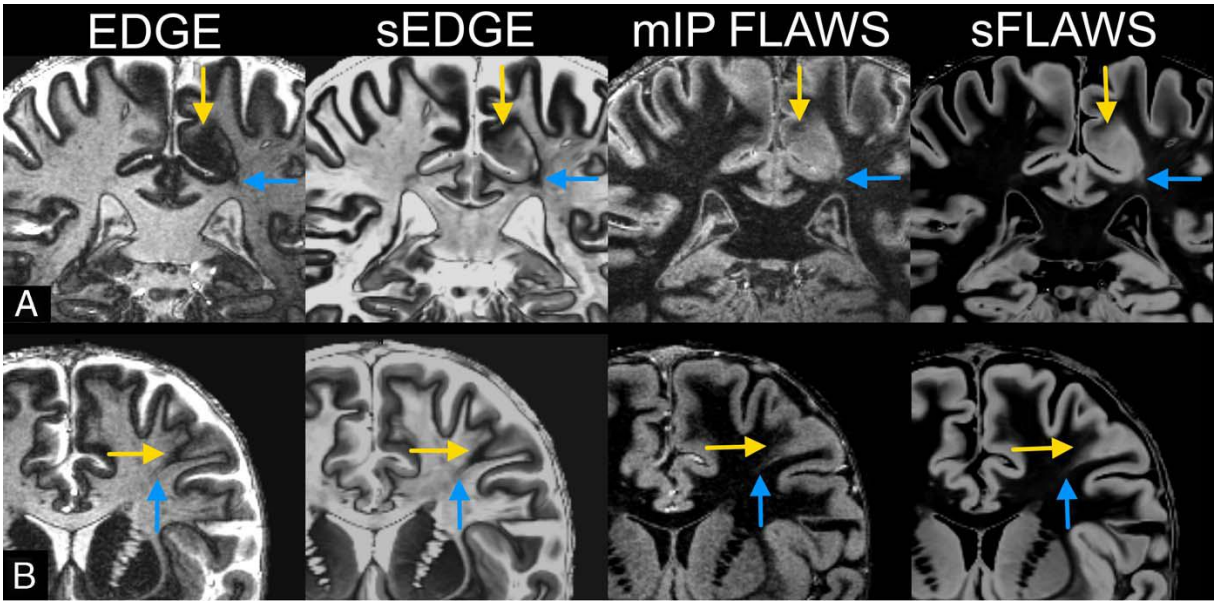

FIGURE 5. 7 T imaging of epilepsy using theMP2RAGE sequence, with improved visualization of epileptic structural focuses (both patients A&B are with FCD type IIb) on synthetic images, when compared with originally acquired images (see arrows). For each patient, fromleft to right: EDGE, sEDGE,mIP FLAWS, and sFLAWS images.

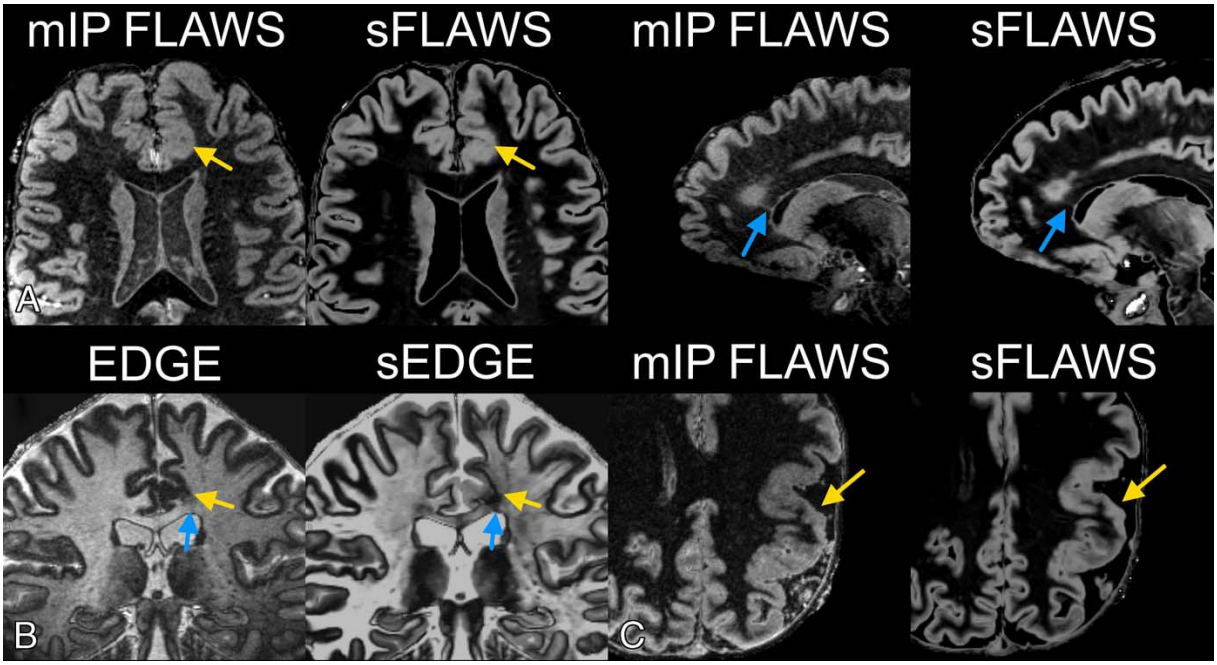

FIGURE 6. Illustrated examples of epilepsy patient data where synthetic imageswere considered slightly inferior than originally acquired images for lesion depiction and delineation. A, FCD type IIb with less obvious cortical thickening (top row, mIP FLAWS vs sFLAWS). B, FCD type IIb with slightly worse lesion-to-WMcontrast (EDGE vs sEDGE). The "transmantle sign" is still visible on these synthetic images (blue arrows). C, Example of a compacted aspect of the parenchyma involved in polymicrogyria (mIP FLAWS vs sFLAWS).